Supplement of Atmos. Chem. Phys., 18, 11991–12010, 2018
https://doi.org/10.5194/acp-18-11991-2018-supplement

Atmospheric Chemistry and Physics
Open Access
EGU

Supplement of

Characterizing the evolution of physical properties and mixing state of black carbon particles: from near a major highway to the broader urban plume in Los Angeles

Trevor S. Krasowsky et al.

Correspondence to: George Ban-Weiss (banweiss@usc.edu)

S1.1 Details on carrying out the LEO-fit method using the PSI Toolkit

Under the LEO-fit tab the first step is to choose "get beam and PSD properties". For this step, we chose scattering low gain (SCLG) for the scattering channel to be used and split low gain (SPLG) for the split detector channel to be used. The split detector helps determine the position of an individual rBC-containing particle within the laser beam. We used the default "minimum peak height to be considered" of 1600 with 40 "points before the peak center to be considered". Upon completion of this step, a "LEO_BeamShapeStats" plot should display a perfect Gaussian response with a shown split detector position. A second output of the PSI-TK is a plot titled "LEO_BeamFWHM_and_SplitTime_Graph". The full width at half maximum for our analysis was approximately 8 μs with a split point to beam center delay time of approximately 4 μs. The second step is to perform the "LEO trace analysis". The fast LEO fit with 3 points was used for our analysis using the SPLG channels for PSD split position. For this section, the PSI-TK will prompt the selection of the "BeamAndCalib" folder within the "LEO" folder of the IGOR Pro data browser. We only fit the scattering low gain data and split low gain data by selecting the "fit SCLG" and "fit SPLG" boxes in the PSI-TK. We concurrently selected "run LEO post processing," which causes "verification of optical sizing" to be performed at this time. The broadband high gain broadband low gain combined signal (BHBL) for the "incandescence channel for BC cores" was selected along with RI=2.26+1.26i for rBC cores and RI=1.50+0i for "Mie data for coated BC core" based on previous literature (Taylor et al., 2014;Moteki et al., 2010; Dahlkötter et al., 2014; Gao et al., 2007). Excellent linear agreement should be found on the PSI-TK outputted plot entitled "LEO_verification_SCLG_vs_SCLG." If

necessary, adjustments can be made based on the given SP2 configuration and the "slope fudge factor".

S1.2 Review of methods in past studies that determine rBC mixing state using the SP2

Here we review past literature that determines rBC mixing state using the SP2. Taylor et al. (2014) investigated rBC wet removal in biomass burning plumes to help constrain rBC radiative forcing estimates. Along with measurements of rBC core size and removal efficiency, the mixing state for 130−230 nm rBC cores was measured using the LEO method with parameters similar to many other studies reported here. They used the scattering signal up to 5% of peak intensity to reconstruct the Gaussian scattering signal. Coating thickness was quantified using Mie calculations with an assumed core refractive index of RI=2.26+1.26i at 1064 nm based on previous work by Moteki et al. (2010), and an assumed shell (or coating) refractive index of RI=1.5+0i. Results from this study demonstrated more efficient scavenging of larger rBC cores with thicker coatings. Liu et al. (2014) measured size distributions, performed a source apportionment analysis, and characterized the mixing state of rBC-containing aerosols in London as part of the Clean Air for London project. To perform the mixing state analysis, Liu et al. (2014) used the LEO method with 1 to 5% peak laser intensity for rBC cores ranging from 100−200 nm with the same refractive indices as Taylor et al. (2014). Results showed that traffic-related rBC-containing particles exhibited very thin coatings with remarkably similar rBC core size distributions for summer and winter measurements (Liu et al., 2014). Laborde et al. (2013) investigated the relationship between hygroscopicity and black carbon mixing state during the wintertime in suburban Paris for rBC core diameters in the range of

180−220 nm and 240−280 nm. The LEO method was applied using up to 1% of peak laser intensity to reduce the chance of including the vaporization signal when performing the Gaussian fitting, effectively using much less of the initial scattering signal than Taylor et al. (2014). Results from Laborde et al. suggest that particles emitted by traffic have essentially no coatings (<10nm), and that as coatings increase in size, the rBC cores become more spherical, demonstrating the influence of coatings on rBC morphology. Schwarz et al. (2008a) measured mass, mixing state, and optical size of individual rBC-containing particles. The LEO method was used to compare the mixing state of urban and biomass burning emissions of rBC cores in the size range of 190−210 nm volume-equivalent-diameter (VED). Results indicated that urban rBC-containing particles consistently had smaller rBC core sizes and thinner non-rBC coatings than those in biomass burning plumes. Schwarz et al. (2008b) assessed coatings using the LEO method for measurements in a NASA research aircraft in the tropics over Costa Rica. They found that 200 nm VED rBC cores had mean coating thicknesses of 30 nm. Schwarz et al. (2014) developed a compact humidification system to quantify the hygroscopicity of rBC in relation to coating thickness quantified by the LEO method. This study introduced a unique way to bridge SP2-measured light scattering to aerosol water uptake properties based on Mie and κ-Köhler theory. Dahlkötter et al. (2014) evaluated aerosol properties and rBC mixing state after long-range transport to the upper troposphere using an aircraft during the CONCERT 2011 field experiment. They found coatings to be much thicker than many other studies (i.e. median thickness ranged from 105 to 136 nm depending on the flight). The SP2 settings used by Dahlkötter et al. made measurements sensitive to scattering material in the optical diameter range of 140 to 290 nm. This study showed

that, assuming a homogenous sphere with refractive index of 1.59 + 0.00i versus the previous literature value of 1.50 + 0.00i, produced uncertainty in the range of 5% for a 200 nm particle. Thus, the assumed RI did not vastly impact the computed coating thickness. Their reported LEO coating thickness histogram showed values ranging from 20 to 180 nm for rBC cores in the range of 140 to 160 nm and 180 to 220 nm. Metcalf et al. (2012) performed a study over the Los Angeles basin during the CalNex campaign and evaluated mixing state using both the LEO and lag-time methods. They presented evidence that shifts in the vehicle fleet on weekends can induce more SOA formation and consequently more thickly-coated rBC particles during the weekends. Shiraiwa et al. (2008) assessed the radiative impacts of rBC mixing state in the Asian outflow at Fukue, a Japanese island. They showed that coating thicknesses ranged from 25 to 400 nm with dependence on source region. Measurements made for Asian continental and maritime air masses exhibited a greater shell to core diameter (1.6) than for Japanese and free troposphere air masses (1.3−1.4). For the LEO method, they elected to set the last point of the leading edge of the scattering signal to a triple Gaussian width away from the center position of the Gaussian. As part of the MIRAGE campaign, Subramanian et al. (2010) performed an analysis over Mexico to investigate rBC mixing state and light interactions as it relates to atmospheric transport. Results from this study show relatively more thinly-coated rBC for measurements made within the urban Mexico City area relative to rBC-containing particles measured at locations away from the city where air masses are more aged.

Supplemental Tables and Figures

Table S1. Number fraction of thickly-coated refractory black carbon particles (mean ± standard deviation) for various lag-times (μs) used to process a 1.5 hour subset of our data. The table demonstrates that as the lag-time approaches 3.4 μs, *f* approaches 0.

Lag-Time (μs)	*f* (mean ± standard deviation)
1.0	0.043 ± 0.041
2.2	0.023 ± 0.028
3.0	0.007 ± 0.015
3.4	0.002 ± 0.009

Figure S1. Map of the two measurement sites in our study.

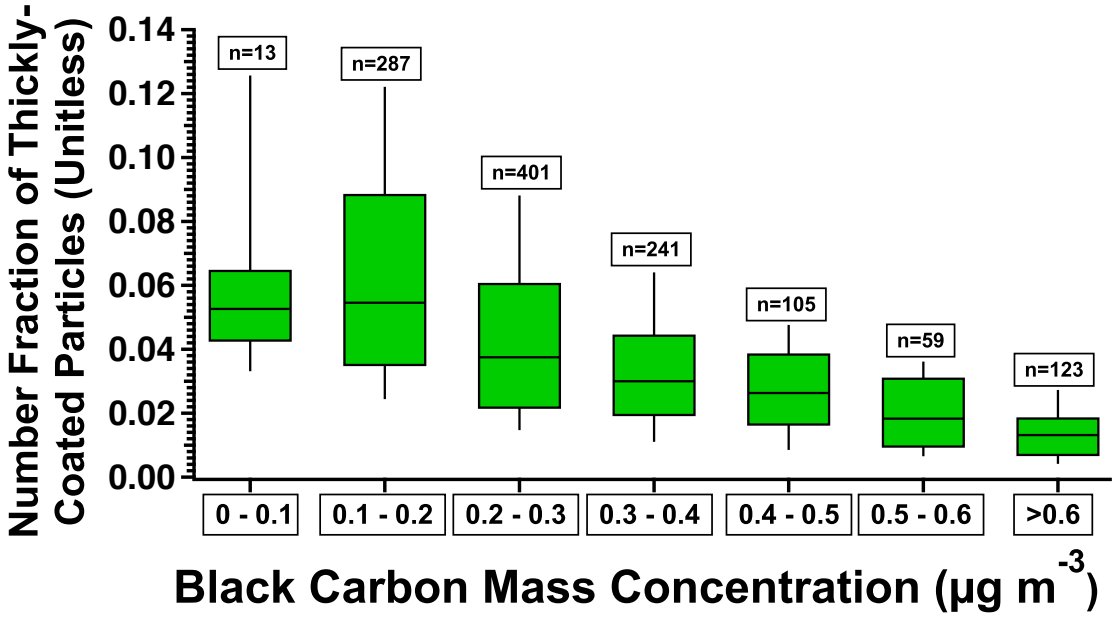

Figure S2. Number fraction of rBC particles that are thickly-coated versus rBC mass concentration (µg m^{-3}) for all measurements made downwind of Interstate 405 in Los Angeles, California. Boxes and whiskers summarize data at 10-second resolution. Boxes depict the 25th and 75th percentiles, whiskers depict the 10th and 90th percentiles, and the horizontal lines within the boxes show the median. The text boxes depict the number of data points in each bin. Data has been filtered to remove 10-second periods where the number fraction of thickly-coated particles was zero. The text boxes indicate the number of data points in each bin.

References

See main body